
Fluid Properties Effects on Sand Production using Discrete Element Method

Seyed Mostafa Seyed Atashi, Kamran Goshtasbi*
and Rouhollah Basirat

Faculty of Engineering, Tarbiat Modares University, Tehran, Iran

(Received: 05/23/2018, Revised: 12/08/2018, Accepted: 12/17/2018)

[DOI: 10.22059/JCHPE.2018.258574.1234]

Abstract

Oil production may be accompanied by Sand Production (SP) in the weak sandstone reservoirs. Fluid flow is an important factor in transporting the separated grains and completing the SP mechanism. In this paper, the effect of fluid parameters, fluid flow, and fluid pressure on the SP is investigated by applying the Discrete Element Method (DEM). Parametric studies show that fluid velocity is reduced by increasing the fluid viscosity, leading to a drop in the SP. In the present study, for an accurate investigation and discovering the effects of viscosity and drag force, the boundary conditions were applied to retain the fluid velocity as a constant amount. The results showed that viscosity is directly related to SP. Moreover, we found that when the fluid velocity is high, there would be the possibility of catastrophic production in the reservoirs with a heavy oil fluid. The rock reservoir around the well will be loosened as soon as SP is initiated. The results also indicate that SP has a direct relation with fluid pressure, fluid velocity, and confining pressure.

Keywords

DEM;
Fluid Properties;
Numerical Modeling;
Sand Production

1. Introduction

Sand Production (SP) is referred to small/large quantities of solid grains that transfer to the surface of reservoir fluid. The sand amount can vary from a few grams or less per one cubic meter (m^3) of fluid to the catastrophic amounts that could make the well full-filled [1].

SP is an unwanted product in removing hydrocarbon reserves from the sand reservoirs. This is-

sue is always considered as a continuous challenge in the oil industry. Moreover, it is associated with several problems such as well instability, reducing the permeability of the formation, abrasion of well equipment, and increasing the associated costs. Therefore, SP has been a subject of intense research and experts in recent decades.

In the sandstone reservoirs, some voids are created in the well wall to increase the production level. Such holes are the main oil producers that also control the well stability. SP phenomenon also occurs in these voids. SP mechanism is shown in Fig. 1.

* Corresponding Author.

Tel.: +989123889159

Email: goshtasb@modares.ac.ir (K. Goshtasbi)

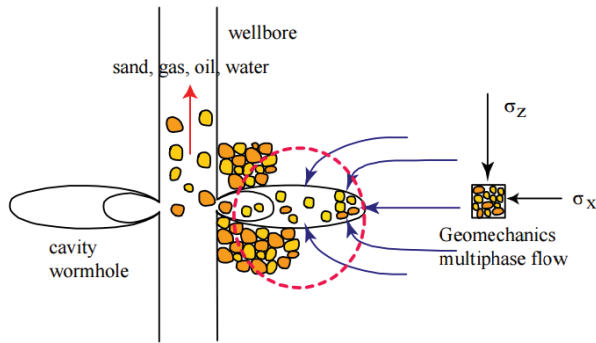


Figure 1. SP mechanism [2]

The combination of both hydrodynamic and geomechanical processes in the failure mechanism, rock erosion, and transferring the grains at the same time has made it very complicated to predict SP procedure. One of the SP study approaches in the well is numerical modeling of reservoir rock with the fluid flow by solving the combined equations of fluid and rock. Several studies have been developed on SP in terms of experimental and numerical models so far.

Nowadays, most SP models have been developed considering the hydromechanical (tensile and shear failure and failure due to the pressure depletion) and erosion mechanisms. Tensile failure occurs when the effective minimum principle stress applying on the rock mass reaches its tensile strength. In comparison, the shear failure occurs when the applied stress on some planes in the wellbore area is higher than their bearing capacity. Pressure depletion causes exertion of effective hydrostatic stresses on rock mass pore structure. Consequently, it breaks and dynamic seepage drag forces cause the internal and external erosion of rock formation during the SP [3].

One of the methods for examining the SP mechanism in the well is the numerical modeling of a reservoir rock, as well as fluid flow with integrated solving of fluid and rock equations. The recent studies conducted on SP can be classified into two major methods: experimental and numerical methods.

Xue and Yuan [4] simulated a well with its reservoir rocks to examine the SP estimation from susceptible areas around the well and to find out how the SP will affect the permeability of reservoir rocks near the well. Fattahpour et al. [5] investigated the effect of grain size on oil well SP using large-scale hollow cylindrical synthetic

samples in the laboratory. They found that for samples with fine grains size, the required confining stress for different sanding levels decreased with an increase in the grain size while for samples with coarser grain size the required stress for different sanding levels increased dramatically with increasing the grain sizes.

Li et al. [6] developed a sand control screen pipe in unconsolidated sandstone reservoirs by combining swellable packers, installing different sized nozzles, and assorting corollary tools. They showed that, compared to conventional screen pipe, sand control screen pipe completed horizontal wells raises in a much slower way.

Ghassemi and Pak [7] simulated an SP using a two-dimensional numerical modeling based on Lattice Boltzmann method and Discrete Element Method (DEM). They found that the magnitude of sand production strongly depends on the flow rate and also the confining pressure (i.e., in-situ stresses). Kaffash and Shadizadeh [8] developed a model for SP rate prediction by coupling fluid flow, particles erosion, and mechanical deformation using finite difference method (FDM). Shirinabadi et al. [9] investigated the SP mechanism in the loose and fractured formations by fabricating a new apparatus for reservoir simulator. They presented a new relation for predicting the SP by applying experimental test results as a function of injected fluid pressure, sand particles diameter, fluid density, and axial force applied to the apparatus. Considering that the numerical finite element methods (FEMs) could neither separately show the particles movement nor simulate the fluid flow in a porous media, several shortcomings are expected in this regard. Hence, a sandstone reservoir was simulated using a DEM in PFC^{3D} software to accurately examine the SP mechanism in an oil well.

2. Discrete Element Model

2.1. Particle-Flow Model

A general particle-flow model simulates the mechanical behavior of a system consisting of a collection of arbitrarily shaped particles. The model is composed of distinct particles that displace independent of one another and interact only at contacts or interfaces between the particles. Newton's laws of motion provide the fundamental relationship between particle motion and the

forces causing that motion. The force system may be in static equilibrium, or be in a state that cause the particles to flow. PFC^{3D} provides a particle-flow model having the following assumptions:

- The particles are treated as rigid bodies.
- The contacts occur over a vanishingly small area.
- Behavior at the contacts uses a soft-contact approach where the rigid particles are allowed to overlap one another at contact points.
- The magnitude of the overlap is related to the contact force via the force-displacement law, and all overlaps are small in relation to particle sizes.
- Bonds can exist at contacts between particles.
- All particles are spherical. However, the clump logic supports the creation of super-particles of arbitrary shape.

The assumption of particle rigidity is a good one when most of the deformation in a physical system is attributed to the movements along interfaces. The deformation of a packed-particle assembly (or a granular assembly such as sand), as a whole, is well described by this assumption because the deformation results primarily from the sliding and rotation of the particles as rigid bodies and the opening and interlocking at interfaces, rather than from individual particle deformation. It has to be noted that the precise modeling of particle deformation is not necessary to obtain a good approximation of the mechanical behavior for such systems.

2.2. Fluid flow motion or hydrodynamics

The Navier-Stokes equations are used for modeling of fluid flow between particles. Eq. 1 shows fluid movement in a porous medium. The effect of porosity in this medium and mass conservation equations for an incompressible fluid in a porous medium are presented by Eqs. 1 and 2 [10].

$$\rho_f \frac{\partial \epsilon \bar{v}}{\partial t} + \rho f \bar{v} \cdot \nabla (\epsilon \bar{v}) = -\epsilon \nabla p + \mu \nabla^2 (\epsilon \bar{v}) + \bar{f}_b \quad (1)$$

$$\frac{\partial \epsilon}{\partial t} + \nabla (\epsilon \bar{v}) = 0 \quad (2)$$

where ρ_f is the fluid density, ϵ is the porosity, p is the fluid pressure, μ is the dynamic viscosity of the fluid, \bar{f}_b is a body force per unit volume, and \bar{v} is the fluid velocity. Porosity as a parameter related to location and time is defined as follows:

$$\epsilon = 1 - \frac{V_p}{V} \quad (3)$$

where V is the volume of a fluid element and V_p is the total volume of all particles contained within that element.

2.3. Fluid and particle interaction forces

Fluid acts two forces on the object body, which is located through the fluid movement path. The first one is lifted force, which applies to the fluid flow movement in the perpendicular direction. The second one is drag force that applies to the particles in direction of flow (Fig. 2). The drag force causes reduction of fluid flow in a porous media, such as water flow inside the pipes, which can cause a pressure drop in the fluid flow. The drag force is applied to the particle body. When this force exceeds the resistant forces applied to the particles, it will make the particles to move.

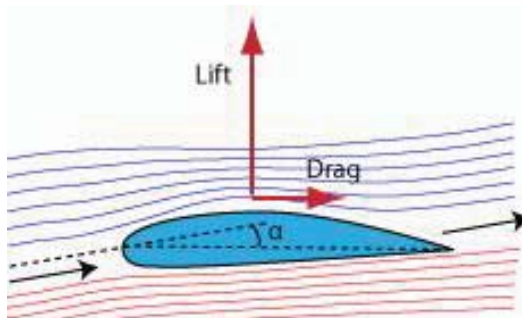


Figure 2. Forces applied to the media particles by the fluid

It should be noted that drag force is generated due to the velocity difference between solid and fluid. Therefore, if there was no motion, drag force would not be created. The amount of drag force in the fluid flow depends on object geometry and fluid viscosity. The geometry causes changes in the flow pressure at the back and front of objects, which is known as the compressive drag force. Viscosity, on the other hand, creates shear stress and viscous drag force while contacts

with the fluid and wall or the object free surface. The drag force applied to individual discrete particles is [10]:

$$\vec{f}_{drag} = \frac{4}{3}\pi r^3 \frac{\vec{f}_b}{(1-\epsilon)} \quad (4)$$

where r is the particle radius. The drag force applied by the particles to the fluid in each fluid element is defined as:

$$\vec{f}_b = \beta \vec{U} \quad (5)$$

where β is a coefficient and U is the average relative velocity between the particles and the fluid. Following Tsuji (1993), the coefficient β is calculated in one of two ways, depending on the porosity of the fluid element. The β is calculated by Eq. 6 for low values of porosity ($\epsilon < 0.8$). The relation is derived by the pressure drop observed in flow through porous materials.

$$\beta = \frac{(1-\epsilon)}{d^2 \epsilon^2} [150(1-\epsilon)\mu + 1.75\rho_f d |\vec{U}|] \quad (6)$$

where μ is the dynamic viscosity of the fluid, ρ_f is the density of the fluid, and d is the average diameter of the particles occurring in the element. The total force exerted by the fluid on the particle is the sum of the drag force and the buoyancy force:

$$\vec{f}_{fluid} = \vec{f}_{drag} + \frac{4}{3}\pi r^3 \rho_f \vec{g} \quad (7)$$

where g is gravity acceleration.

2.4. Algorithm and coding

Modeling was conducted using the PFC^{3D} software and coding. Every code always requires an appropriate algorithm. The algorithm is a calculation procedure that takes a variable or a complex as an input data and turns it to an output one through some computational stages. Algorithm design and build is the core of programming activities. Defining variables and stage-wise design are very important for each algorithm. Fig. 3 shows the SP modeling flowchart. Each algorithm computational stage includes a main function that consists of some sub-functions and loops.

3. Verification

Numerical simulation is always preferred compared to the laboratory and site methods in

terms of economic and time considerations. However, to validate the obtained results, it is necessary to compare them with the experimental data. In the following, the results of numerical modeling are compared with experimental data in order to validate the model.

3.1. Introduction of the experimental model

The reservoir simulator is a cylindrical chamber that contains a well at the center. Fig. 4 shows a test apparatus and the way a hole is drilled inside the well wall.

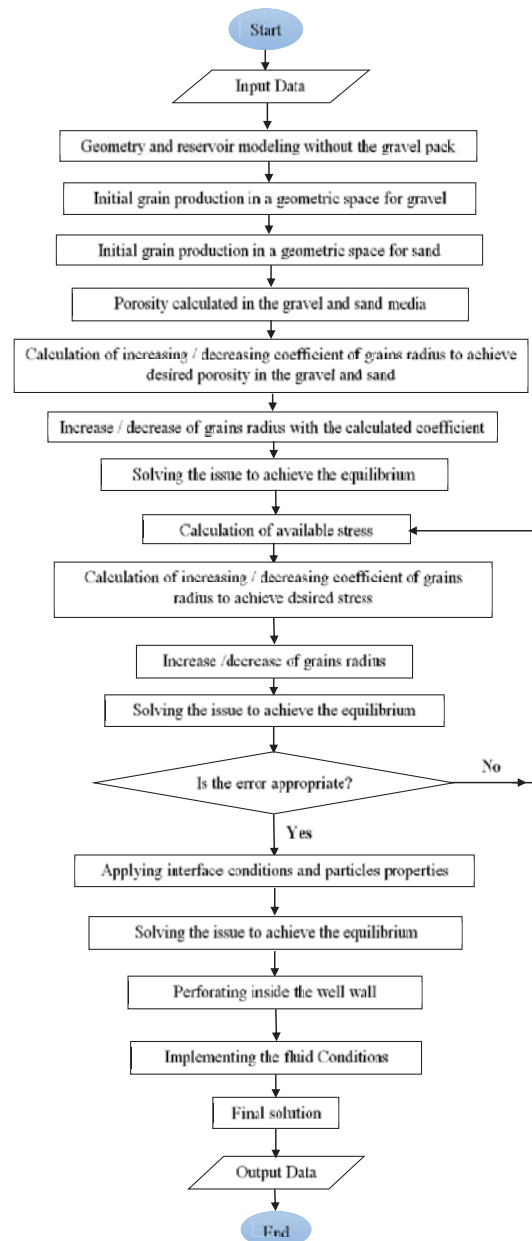


Figure 3. SP modeling flowchart by using DEM



Figure 4. Chamber of reservoir simulator with the cover and interior components [9]

A steel plate is located on the sand sample, wherein the stress of sandstone reservoir is controlled using a hydraulic jack installed at the top. Lubricating inside the cracks around the steel plate prevents fluid and sand particles to exit from the apparatus top. Input pressure is a constant value during the test. This apparatus simulates a loose sandstone formation (without cohesion strength between particles) that is located under an impermeable layer (caprock). The fluid used in the test contains water with a viscosity of 1 cP and has a density of 24 kg/m³ [9].

3.2. Specifications of a numerical model for verification

Regarding the geometry of the experimental model, some issues such as well core types, properties of the sand particles, and fluid flow were stimulated in the numerical model. Fig. 5 shows the geometry specifications of the numerical model. Also, Table 1 presents the properties of used particles as verification.

The numerical model is simulated for both conditions (with and without gravel pack). Fig. 6 shows two numerical models (with and without gravel pack) for verification.

3.3. Comparing results

SP average rate is calculated through five tests for both conditions of with and without gravel pack. Next, the SP rate average in tests is compared with the numerical results. SP is considered zero for the condition with gravel pack in both numerical model and experimental data. The experi-

mental tests without gravel have different SP but close to each other. By an average of these values, the main SP rate was calculated to be 4.22 gr/s for the experimental tests. SP in the numerical model is shown in Fig. 7. Moreover, the SP rate comparison of the two presented models and experimental data is presented in Table 2.

Table 1. Properties of the particles used in a numerical model for verification

Parameter	Value
Particles radius	1-2 mm
Gravel particles radius	2.34-4.5 mm
Number of particles without gravel in model	55322
Number of particles with gravel in model	52853
Normal stiffness	10 ⁸ N/m
Initial porosity	20 %
Shear Stiffness	10 ⁸ N/m
Particle density	2650 kg/m ³
Fluid density	1000 kg/m ³
Fluid dynamic viscosity	1 cP
Pressure of entering fluid	200 kPa

Table 2. Comparison results of SP rate experimentally/numerically (gr/s)

Model	Experimental	Numerical
With gravel pack	0	0
Without gravel pack	4.22	4.33

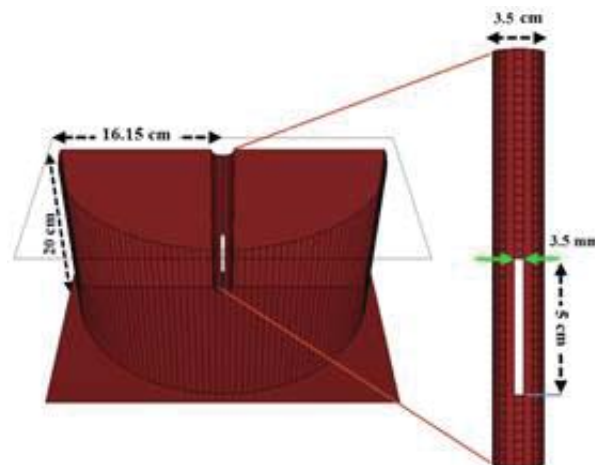


Figure 5. Geometry properties of a numerical model for verification

According to Table 2, the results of numerical models are consistent with the experimental data.

However, there is a little discrepancy because particles are considered fully spherical in the numerical model but the sphericity in the experimental data is 0.7.

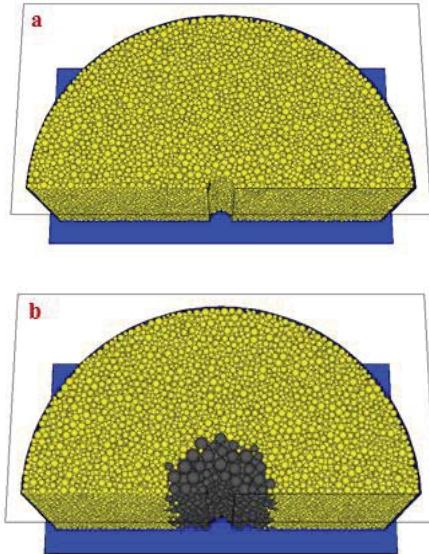


Figure 6: Numerical models in two conditions: a) without gravel pack and b) with a gravel pack

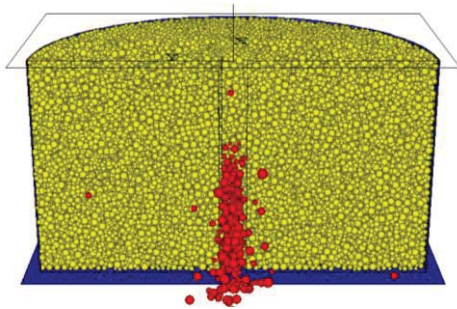


Figure 7. SP in Numerical model

4. Three-dimensional Modeling

Fig. 8 shows the model geometry and the lattice wall (holes inside the wall). Considering that the PFC^{3D} software is not capable of building a curved wall, a large number of walls are used in the route of both reservoir and well cylindrical curvature. Needless to say, the number of walls is customizable.

According to Fig. 8, the diameter of the sandstone reservoir is 60 cm, where a well is drilled through it with a diameter of 6 cm and height of 10 cm. The reservoir diameter is chosen 10 times larger

than the well diameter to reduce the structural effects of well to zero and also reach the zero possibility of SP from the boundary of the well. In the solving process, the amount of force applied to sand grains by the fluid is calculated at each fluid time step. The sand grains move if the movement resultant forces overcome the retaining forces of particles in their position.

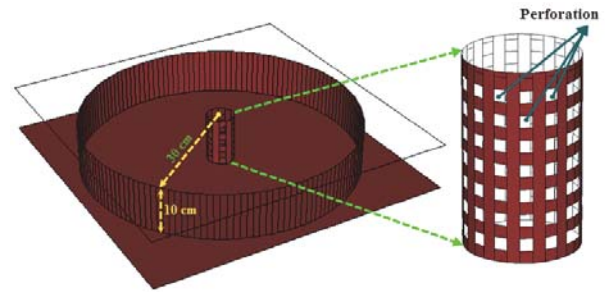


Figure 8. Model Geometry

If this movement extends to the well and sand grains along with fluid entrance to the wellbore, SP initiates. In this simulation, the particles are changed with entering grains to the well. Then, the size and weight of the particles are calculated. Fig. 9 shows the fluid flow in the well and sand production phenomena. It should be noted that to reduce the run time of models a semicircular sector (half of the well) is simulated.

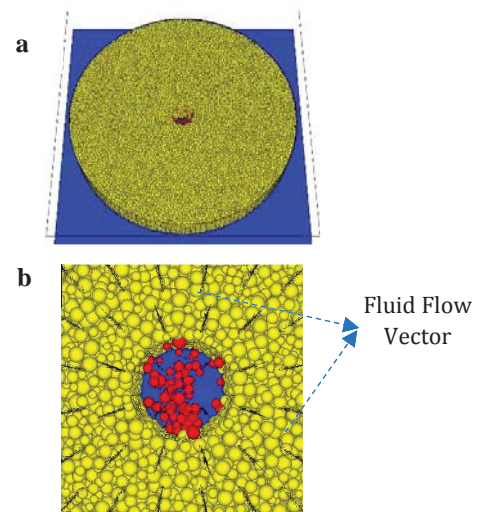


Figure 9. a) A complete view of the reservoir and b) A near view of sand production in the well

5. Sensitive Analysis

Different models with varying conditions were simulated to examine the fluid parameters on SP. In examining any specific parameter, other parameters were considered as a constant value, to make SP changes dependent on the only desired parameter. Considered parameters for sensitivity analysis are as follows:

- Fluid pressure
- Properties related to the type of fluid (viscosity and density)
- Input flow rate to the well

5.1. Effect of fluid pressure on SP

To examine the effect of fluid pressure on SP, four pressures of 100, 200, 400, and 1000 kPa were implemented in the reservoir margins to the well under fluid boundary conditions. SP in different conditions is shown in Figs. 10 and 11.

Petroleum reservoirs are media with high fluid pressure. A level with zero pressure (atmospheric pressure) occurs in such reservoirs through well drilling. In the reservoir, pressure discrepancy is the main factor in fluid movement toward the well. In this situation, the more the pressure discrepancy is, the more fluid motion velocity happens in the reservoir. So, by increasing the velocity, a compression drag force caused by the fluid motion is applied to the particles in a porous medium. Therefore, as shown in Figs. 10 and 11, increasing the fluid pressure will increase the SP intensity in the well. Contact forces will be also reduced by increasing SP so that a loose area is developed around the well.

To examine the fluid pressure effects on SP more accurately, the curves related to the sand cumulative production and sand production rate, for all four models, are shown in Figs. 12 and 13 respectively.

According to Fig. 13, SP rate in the well reaches a constant value under different pressures. This constant value will increase in higher pressures. So, the curves of sand cumulative production (Fig. 12) always have a distance from each other with a constant gradient. In other words, SP discrepancy in the well is being constantly increased with increasing the fluid pressures.

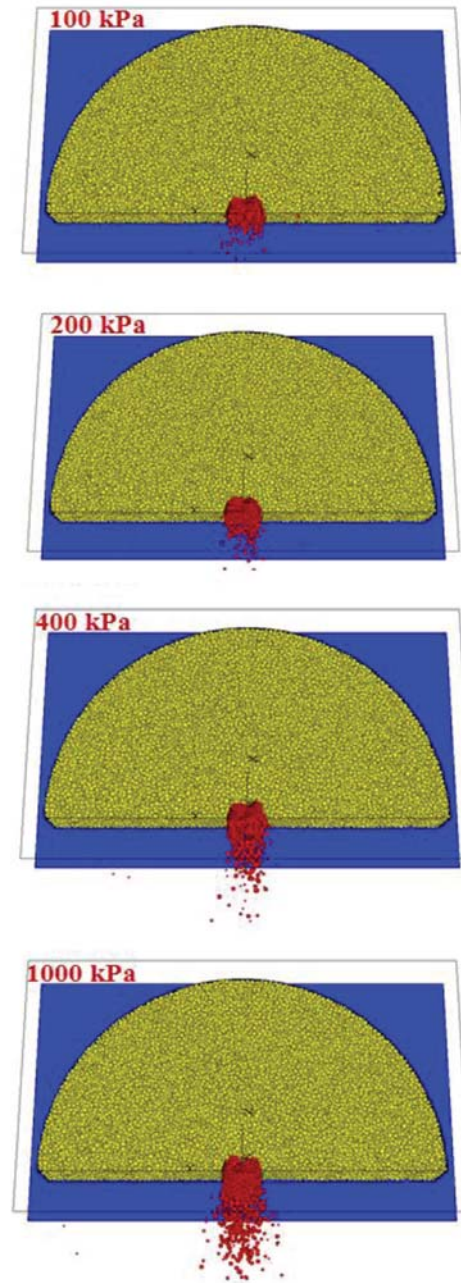


Figure 10. SP in numerical models with different fluid pressures

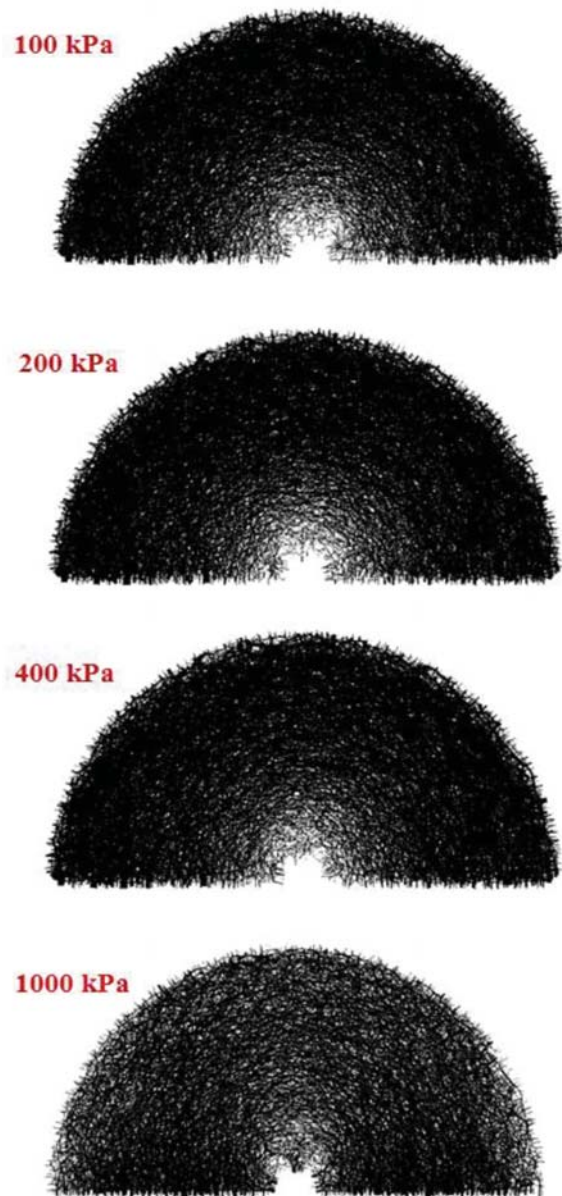


Figure 11. Contact forces in numerical models with different fluid pressures

5.2. Effect of fluid viscosity and density on SP

Considering the changes in fluid viscosity and density with each other, a sensitivity analysis was performed on these fluid parameters. For this purpose, 5 fluids with different viscosities and densities were considered, and SP value and rate were studied for each model. Fluid properties are presented in Table 3.

Viscosity changes affect the force that the fluid act on the sand particles in two ways. The first one

occurs in the viscous drag force, which increases by increasing the viscosity and density of the fluid (as described in Eq. 6). The second one is related to the fluid viscosity effect on velocity in a porous media. In this case, fluid velocity is decreased by increasing the viscosity. Therefore, the compressive drag force is decreased by decreasing the fluid velocity. Since the effects caused by fluid velocity in a compressive drag force (applied to the particles) are more than viscosity in a drag force, the resultant force from the fluid to the particle in a reservoir rock reduces by increasing the viscosity. The results extracted from 5 models run by different viscosities represent this issue effectively. As shown in Fig. 14, SP is reduced in a well by increasing the viscosity value. According to Fig. 14, SP is slightly reduced with a small increase in the fluid viscosity (changes from water to the medium oil, 1-10 cP); however, SP has a significant reduction in heavy oil (viscosity 3000 cP).

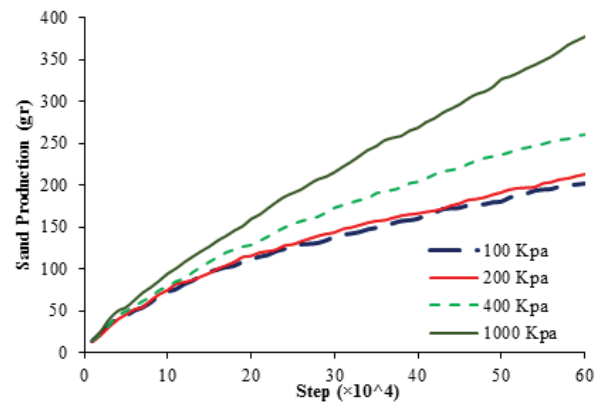


Figure 12. SP values under different fluid pressures

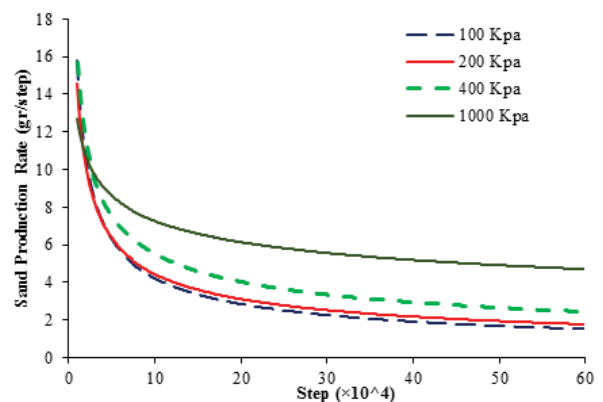


Figure 13. SP rate under different fluid pressures

Table 3. Fluid properties

Row	Fluid type	Viscosity (cP)	Density (kg/m ³)
1	Water	1	998/23
2	Light oil 1	3	825
3	Light oil 2	6	850
4	Medium oil	100	880
5	Heavy oil	3000	965

In addition, according to Fig. 15, it is clear that SP reaches a constant value in all models, suggesting an effective continuous production. Three other models were run in the reservoir to gain a better understanding of the viscous drag effects.

In new models, the fluid boundary conditions were applied in a way to flow the fluid into the well at the same velocity with varying viscosities. The fluid flows in three models include light oil, medium oil, and heavy oil. Figs. 16 and 17 respectively show SP value and rate in each model.

Eq. 4 shows that drag force on the particle depends on two values: porosity and volume forces. Drag force always increases on particles as the porosity increases in the reservoir rock. The important point gained in this research is the SP rate in a reservoir containing heavy oil. According to Fig. 17, SP rate always increases when both the viscosity and velocity of fluid are high, which leads to a risk of instability and catastrophic production.

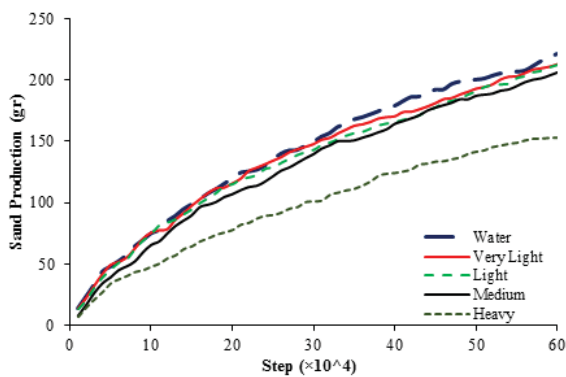


Figure 14. SP under different viscosities

5.3. Effect of fluid flow rate on SP

To investigate the flow rate on SP in a well, the fluid with three macroscopic velocities of 0.1, 0.3, and 0.6 mm/s were allowed to enter the sandstone reservoir from around the well during im-

plementing the fluid boundary conditions. Based on the reservoir geometry dimensions, the area of the reservoir wall will be 0.188 m². Finally, according to the relation of flow rate with surface area and velocity ($Q=A \times V$), the fluid flow rate in three models are 18.8, 56.4, and 112.8 cm³. Figs. 18 and 19 respectively show SP and SP rate in each model.

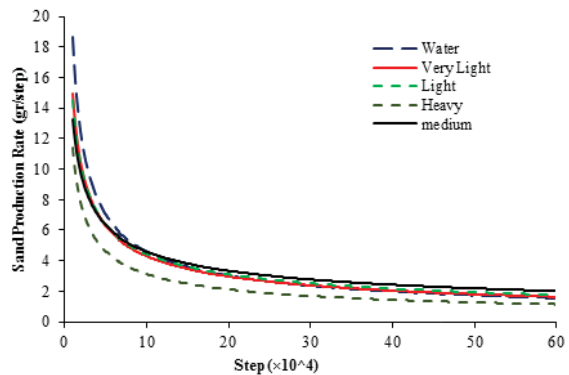


Figure 15. SP rate under different viscosities

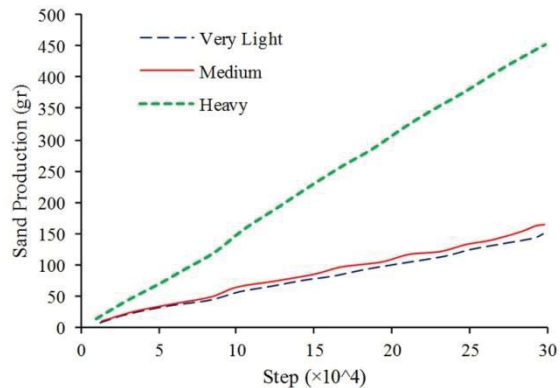


Figure 16. SP with different viscosities and a constant fluid velocity

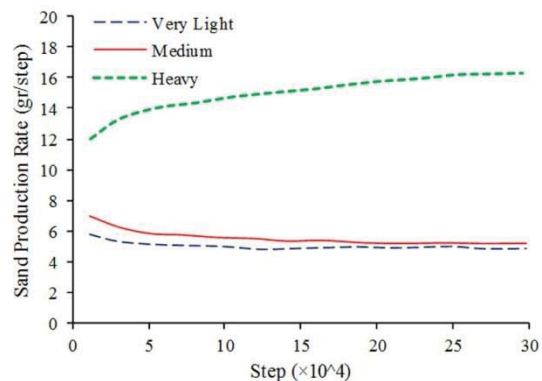


Figure 17. SP rate with different viscosities and a constant fluid velocity

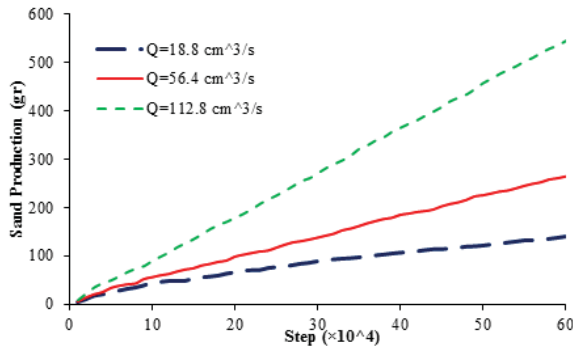


Figure 18. SP with different flow rates

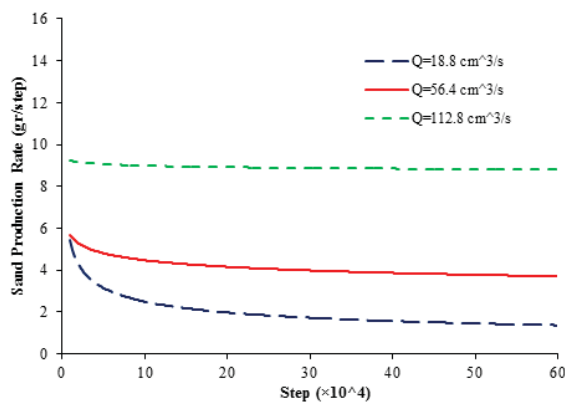


Figure 19. SP rate with different flow rates

According to Fig. 17, SP is enhanced by increasing the rate of flow into the reservoir. Unlike the previous models, the constant rate of fluid flow has caused the SP rate to reach a constant value quickly. Therefore, it can be concluded that constancy of fluid velocity in the reservoir means that drag force is constant on the particles. In this way, it is possible to overcome the SP problem by controlling this parameter in the reservoirs. It should also be noted that in high SPs, difference in value of SPs related to high and low flow rates is constantly increasing because the gradient of cumulative production curve is determined by SP rate values.

6. Conclusions

In this paper, the effects of flow rate and fluid properties on sand production (SP) phenomenon are studied in the sandstone reservoirs, oil wells, and drilled wells by simulating in PFC^{3D} software. The major findings of this study are as following:

- Results from numerical modeling were compared with experimental data. SP is zero in both numerical modeling and experimental data, which have gravel as a preservative. In cases, the well has no gravel pack, SP rate in the numerical model is highly consistent with the experimental results.
- The cumulative amount of SP is reduced by increasing the viscosity in the sandstone reservoirs with a constant pressure gradient.
- In sandstone reservoirs, if the fluid velocity is constant for different viscosities, SP rate increases as the viscosity increases.
- In heavy oil reservoirs, catastrophic production is possible if the fluid velocity is high.
- The reservoir rock is loosened around the wellbore when SP initiates. Also, the loose area will develop by increasing the SP.
- SP is enhanced by increasing the fluid pressure gradient on the edge of the reservoir. SP rate also has a higher value in high fluid pressures, suggesting that SP difference is constantly increasing for the gradient of different pressures.
- The constancy of fluid velocity in the reservoir is always associated with a constant SP. Generally, SP has a direct relation with the output rate. Therefore, by controlling the rate of input flow to the well, the fluid velocity can also be controlled in the reservoir, which allows controlling the SP in the well.

References

- [1] Fjar, E., Holt, R. M., Raaen, A. M., Risnes, R. and Horsrud, P. (2008). *Petroleum Related Rock Mechanics*, 2nd. Ed. Elsevier, Burlington.
- [2] Wang, J., Walters, D., Wan, R. G. and Settari, A. (2005, January). "Prediction of volumetric sand production and wellbore stability analysis of a well at different completion schemes." In *Alaska Rocks 2005, The 40th US Symposium on Rock Mechanics (USRMS)*. American Rock Mechanics Association.
- [3] Ranjith, P. G., Perera, M. S. A., Perera, W. K. G., Choi, S. K. and Yasar, E. (2014). "Sand production during the extrusion of hydrocarbons from geo-

logical formations: A review." *Journal of Petroleum Science and Engineering*, Vol. 124, pp. 72-82.

[4] Xue S, Yuan Y. (2007). "Sanding Process and Permeability Change." *Journal of Canadian Petroleum Technology*, Vol. 46, No. 4, pp. 33-39.

[5] Fattahpour, V. Moosavi, M. and Mehranpour, M. (2012). "An experimental investigation on the effect of grain size on oil-well sand production." *Petroleum Science*. Vol. 9, Nol. 3, pp. 343-353.

[6] Li, L. C., Yang, S. L. and Chen, H. (2013). "Water and Sand Control Technology Successfully Applied in Jidong Oilfield: A Case Study." *Energy Sources, Part A: Recovery, Utilization, and Environmental Effects*, Vol. 35, No. 24, pp. 2294-2301.

[7] Ghassemi, A. and Pak, A. (2015). "Numerical simulation of sand production experiment using a coupled Lattice Boltzmann-Discrete Element Method." *Journal of Petroleum Science and Engineering*, Vol. 135, No. 218-231.

[8] Kaffash, A. and Shadizadeh, S. R. (2015). "A New Method for Modeling the Rate of Sand Production." *Energy Sources, Part A: Recovery, Utilization, and Environmental Effects*, Vol. 37, No. 19, pp. 2081-2091.

[9] Shirinabadi, R. Moarefvaand, P. Goshtasbi, K. and Ahangari, K. (2016). "The physical and numerical modeling of sand production and gravel pack in oil wells by designing and manufacturing the machine and presenting a relation estimating sand production rate." *Journal of Mining Science*, Vol. 52, No. 2, pp. 300-312.

[10] Itasca consulting group, Inc. (2012). PFC3D (Particle Flow Code in 3 Dimensions) version 4 and 5 User Manual.